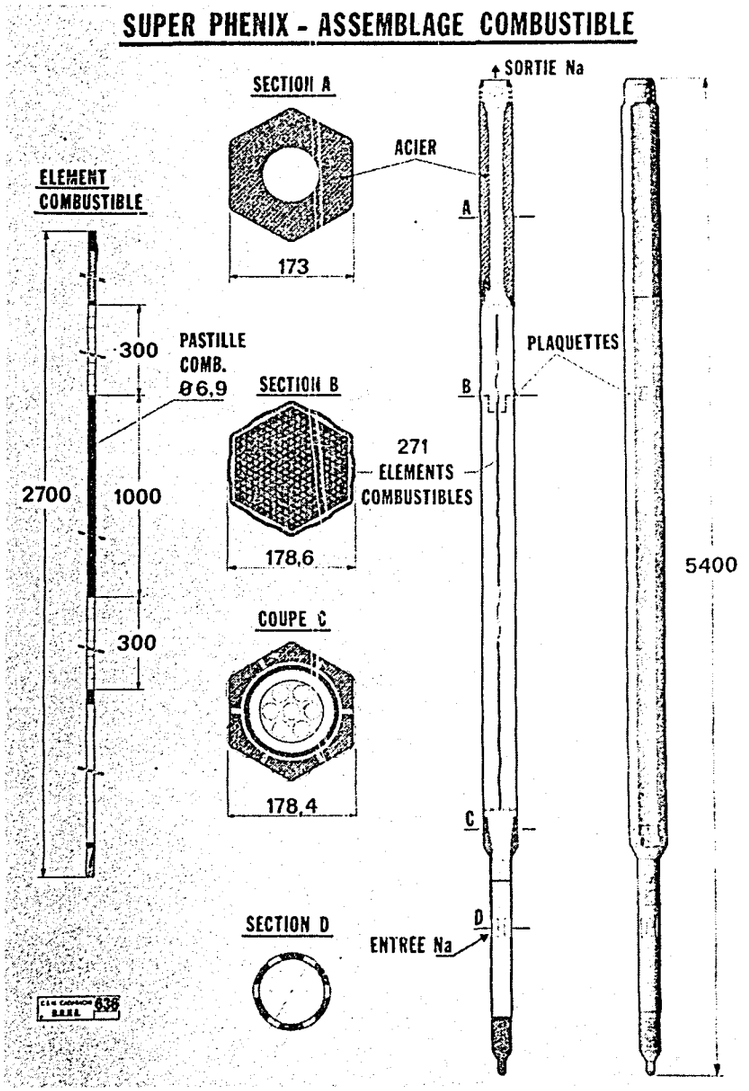

FIG. 7.

FIG. 8. SUPER PHENIX
FLOW REGULATION SYSTEMS
CAVITATION STUDIES

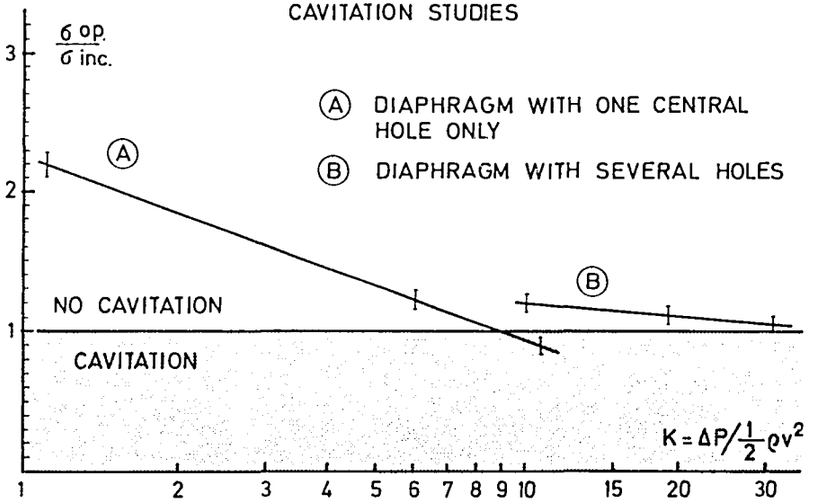

3 " The Onset of Cavitation in Pressure Dropping Devices in Water and Sodium, " A.E. COLLINSON, U.K.A.E.A., U.K.

1. INTRODUCTION

It is necessary to develop pressure dropping devices for the control of flow in LMFBR sub-assemblies and other components in and around the core. It is generally required that these devices should have a high flow rate, high pressure loss, occupy a very limited space and not be prone to cavitation. If it is intended to detect coolant boiling acoustically then it is important that there should be no cavitation noise background which would result in reduced sensitivity of the boiling noise monitor.

This paper describes a series of tests conducted in water and sodium for the development of cavitation noise-free pressure dropping components for PFR. Initial tests were conducted on single ISA nozzles, being followed by the more practical multi-hole nozzle plates and wire meshes. Tests of a plug in a cylindrical bush are described as an example of a sealing unit with an annular gap.

2. TEST PHILOSOPHY

The conduction of a sodium test programme is tedious and time consuming. It was therefore decided to perform the majority of tests in water using

selected sodium tests in order to endorse components developed in water. It was assumed that if one design of pressure dropper had a better water cavitation performance than another, then the same would apply for sodium. Sodium tests were conducted when a component had already been optimised using water. It was considered that, in the absence of cavitation noise, erosion would not be a problem.

3. EXPERIMENTAL FACILITIES

a. Water Cavitation Loop

Fig 1 shows a flow diagram of the water cavitation loop used for the majority of the tests described later. The basic test section (fig 2) is a tube 150mm bore 3.6m long constructed from perspex blocks with thick walls and flat outer wall faces to enable good viewing of items under test. The six pumps can circulate the distilled water at flows up to 35 l/s with a pressure drop of 700 kN/m^2 or 75 l/s at 1400 kN/m^2. The loop was designed to suppress pump and pipework cavitation. The pumps 1 and 2 are of the sealed rotor type and are situated in a pit 7.5m below the test section. Pipework downstream of the pumps is 100mm bore, the return line being 200mm bore in order to minimise the flow velocities at the low pressure side of the loop. Valves are of the plug type in order to obtain least resistance for the fully open condition. Loop flow is measured using turbine flow meters on the high pressure side, the accuracy being $\pm$ 0.5%. The background loop static pressure can be varied from 0.25 to 14 bar irrespective of the flow by using a vacuum pump on the gas space in a small header vessel or by pressurising a set of pressure accumulators. Water temperature can be varied from 15 to 50°C, heat being derived from the pumps and removed by a heat-exchanger connected to a small forced-draught cooling tower. The dissolved gas content can be reduced to about 0.1% of saturation by boiling a bypass flow in the main header tank.

b. Sodium Cavitation Loop

Sodium tests were carried out on a loop attached to the 450 l/s sodium pump loop at KEML (Ref 1), a schematic diagram being shown on fig 3. The maximum loop flow was 40 l/s with a pressure drop of 350 kN/m^2, the downstream static pressure being limited to the range 0.3 - 1.0 bar by the design of mechanical pump tank. A venturi was used in conjunction with a sodium manometer for the upper end of the flow range, an electromagnetic flowmeter being used otherwise. The test section was fabricated from 150mm bore tube and could be removed from the loop following isolation from the main rig. The loop operating temperature was in the range 200-400°C. Free gas in the system could be settled out in the mechanical pump tank by running the main loop at a low flow. The level of free gas in the system could be roughly varied by injecting gas upstream of the test section, the large bubbles injected being broken down on passing through the pump.

4. DETECTION OF CAVITATION

Cavitation was detected acoustically in all the tests carried out. For water tests either piezo-electric microphones were mounted on the test section wall or hydrophones suspended in the flow downstream of the test section. The sodium test section carried solid steel stubs welded to the wall so that the microphones attached did not operate at an excessive temperature. The associated electronic equipment is outlined in fig 4, being designed specifically for the monitoring of the noise produced at the onset of cavitation. The microphone signal was amplified and filtered, only frequencies > 10kHz being accepted and fed to a discriminator. The discriminator level was set such that, in the absence of cavitation, background flow and electronic noise was eliminated. The resultant signals were displayed on a storage oscilloscope and a scaler unit similar to those used for counting atomic particles. The scaler gave an output which was proportional to the number of cavitation bubble collapses, the corresponding pulse forms being shown on the oscilloscope.

5. EXPERIMENTAL DETERMINATION OF CAVITATION ONSET

Before noise measurements were taken, the loops were operated at constant flow and liquid temperature at a high background pressure in order to minimise the number of free gas bubbles circulating. The background pressure was then lowered in small stages, the scaler output being determined for each step, until cavitation was well developed. A typical characteristic for a nozzle geometry is shown in fig 5, the test fluid being water. The cavitation number σ is defined as

$$\sigma = \frac{P_t - P_v}{DH_t} \quad \text{.....(1)}$$

where P_t is the throat static pressure, P_v the fluid vapour pressure and DH_t the throat dynamic head given by

$$DH_t = \frac{\rho}{2}\left(\frac{Q}{A_t C_A}\right)^2 \quad \text{.....(2)}$$

ρ is the liquid density, Q the volume flow rate, A_t the area of the throat and C_A the area discharge coefficient.

As σ reduced, cavitation commenced as a series of isolated single bubble collapses, becoming more frequent as the pressure was lowered. This region, shown as A-B in fig 5, is referred to as the intermittent region. As the behaviour in this region is intermittent no critical cavitation number can be defined for its onset: at increasing σ events become less and less frequent. At point B the slope of the characteristic suddenly increases, noise becoming continuous as the point C is approached. The region B-C can be identified with visible cavitation at the nozzle throat and an incipient σ_i can be defined by the interception of the lines AB and CB. At D the scaler unit becomes saturated, the noise level being very intense and crackling in nature resulting in test section vibration. At E significant volumes of vapour are formed and the noise becomes reduced in intensity due to the attenuation of sound by the large number of bubbles present. In sodium the region of cavitation onset A-B-C was similar to that for water, but the loop was not operated beyond C because of the danger of vibration or cavitation damage in the test section.

6. TEST RESULTS

a. ISA Nozzle

Initial tests were carried out on ISA nozzles conforming to British Standard 1042, part 1 section 12 (1964), in order that results from the

two test loops could be compared with those of other workers (ie Kobayashi, 1967, ref 2) for a simple standard geometry. Cavitation noise characteristics for nozzles with a throat to upstream area ratio m = 0.05 and a throat velocity V_T = 20 m/s for water at 20°C and sodium at 300°C are shown in fig 6. The incipient cavitation number σ_i for throat cavitation was about 1.0 in each case, but the noise levels for $\sigma > \sigma_i$ differed. This difference is to be expected on account of fluid thermodynamic properties, nucleus population and test section or fluid noise transmissibility. The measurement of cavitation onset using microphone RMS output resulted in similar values of σ_i.

The viariation of σ_i with m for a range of ISA nozzles is shown in Fig 7, results from Kobayashi (1967) also being shown. It should be noted that Kobayashi determined the visible onset of cavitation and that for the REML work σ_i, as determined from the change of slope in the noise characteristic, more or less coincided with σ_i values obtained by observing incipient cavitation at the nozzle throats.

The level of cavitation noise for $\sigma > \sigma_i$ was significantly dependent on the degree of flow disturbance. Careful observation with good lighting showed that a significant part of the water intermittent noise regime could be attributed to visible streaks of cavitation upstream of the nozzle. The introduction of upstream swirl led to a dramatic increase of intermittent noise count-rates with significant noise levels for σ as high as 10. It is probable that the intermittent cavitation noise was due to vortices in the flow. As an eddy or vortex passes towards the nozzle throat its peripheral velocity increases due to conservation of angular momentum resulting in a local pressure depression in addition to the general reduction of static pressure. Cavitation will occur if a suitable nucleus is present in the flow. The more intense the eddy the further upstream cavitation will occur resulting in a larger vapour pocket at the nozzle throat. This behaviour highlights the need for a good upstream flow geometry in any system where cavitation noise is to be kept to a minimum. Cavitation of eddies also occurs downstream of the nozzle in the highly disturbed region produced by the diffusing jet.

b. Multi-hole Nozzle Plates

The space occupied by a pressure dropper can be minimised by using multi-hole nozzle plates with N holes rather than single hole plates. Fig 8 shows some of the multi-hole geometries tested, the inlet curvature in each case conforming to BS 1042 assuming each hole to be served by the same flow area.

Test results for a 19 hole plate with m ~ 0.10 and V_T = 20 m/s in water at 20°C and sodium at 300°C are shown in fig 9. The curves are similar to those found for single nozzles, σ_i being the same for water and sodium. σ_i = 1.5 - 1.6 compares favourably with the value σ_i = 1.6 from fig 7 for a single nozzle with a similar m value.

For all the nozzles tested the noise level was a strong function of throat velocity both for water and sodium. Fig 10 shows curves for a 60 hole plate in water with throat velocities varying from 8 to 25 m/s. There was a distinct tendency for σ_i to increase with increasing V_T in addition to the much higher intermittent event rates for higher velocities. With V_T = 8 m/s cavitation occurred at the throat without being preceded by an intermittent region. The count rates were also very sensitive to temperature both for sodium and water, increasing markedly with rising temperature in the intermittent noise region. No significant variation of σ_i with temperature was detected. The temperature variation could be due to changes of vapour pressure, rig nucleus population, thermodynamic effects or viscous effects. Considering the relatively high throat static pressure in relation to vapour pressure and the small amount of free or dissolved gas present it would seem unlikely that variation in vapour pressure or nucleus population would account for the large changes in noise level observed. On the other hand, viscous effects will occur for vortices such as postulated upstream of nozzle plates. As an eddy or vortex contracts in diameter on passing through a restriction the tangential velocity increases, due to conservation of angular momentum, and the axial pressure falls relative to the static pressure outside the vortex. The increase of tangential velocity is resisted by viscous forces, the lower the fluid viscosity the higher the radial pressure drop across a vortex. As the water temperature increases more vortices in the flow develop axial pressures equal to the vapour pressure in passing the nozzle throat resulting in more cavitation. Fig 11 shows the correlation of count rate with viscosity.

Fig 12 shows the effect of the number holes in a nozzle plate. The plates tested had the same m value and throat velocity, all other test parameters being fixed. σ_i did not vary significantly but intermittent noise levels decreased with increasing N.

c. Wire Meshes

It can be inferred from Fig 12 that if N is large enough the intermittent noise region will be absent. A wire mesh having effectively several hundred perforations with rounded entry approximates to a multi-hole nozzle plate. The cavitation performance of wire meshes with m ~ 0.3 (based on projected throat area) in water and sodium is shown in Fig 13. There was a significant level of background gas bubbles at the start of the sodium test, giving rise to noise levels that only changed slightly with reducing σ. Most of this gas had settled out in the pump tank after 36 hours operation. There was no intermittent noise region for this geometry, cavitation being incipient in both water and sodium for σ_i = 1.0.

d. Narrow Annular Gap

The hydraulic hold-down system for PFR fuel sub-assemblies consists of a cylindrical plug seated in a tube with a small diametral clearance (Fig 14). The full core pressure drop is developed across the plug resulting in high fluid velocities in the eccentric annular gap and possible cavitation at the downstream side. The geometry of Fig 14 was cavitation tested in both water and sodium in special test-sections designed for low flow and high pressure drop. The respective cavitation performances are shown in Fig 15, σ being defined in terms of the mean flow velocity in the annulus and downstream pressure. The onset of cavitation was very sensitive to the presence of trapped debris or surface features such as rough machining marks. With no such defects for water at 20°C cavitation occurred at the end of the parallel portion as shown in Fig 14 with σ_i = 1.05. A small particle ~ 1mm dia trapped close to the downstream edge gave rise to local cavitation with σ_i = 1.5, σ_i for this condition depending on the size and position of the trapped particle. The sodium curve corresponds more to the water condition with the trapped particle. However, it was not possible to show whether debris was trapped for the sodium test so it is possible that σ_i could be different in water and sodium. At $\sigma > \sigma_i$ there was no intermittent cavitation for water or sodium; for the sodium case a small amount of background gas was present. The root mean square

(RMS) microphone output for the sodium test is compared with the results of the counting technique in Fig 16. The change in slope of the two curves occurs at the same σ_i; RMS measurements are satisfactory for the determination of σ_i but are of little use for the assessment of intermittent noise encountered with nozzles.

Fig 17 shows the frequency spectrum from a microphone mounted on a cylindrical steel stub when cavitation was continuous. The spectrum was recorded using a Ubiquitous frequency analyser, type UA-500-A, and was typical of the tests conducted. The peaks are considered to be due to the test-section, microphone and mounting stub resonances rather than to the cavitation itself. The cavitation spectrum would appear to be fairly broad band in the range 0-50kHz.

7. CONCLUSIONS

a. In general well degassed water at 20°C appeared to be a reasonable medium for modelling cavitation onset for ISA nozzle plates and wire meshes in sodium at 300-400°C.

b. For nozzle plates two distinct regions of cavitation occurred. At higher cavitation numbers $\sigma > \sigma_i$ intermittent cavitation took place in eddies generated both upstream and downstream of the nozzles whereas for $\sigma < \sigma_i$ continuous cavitation occurred at nozzle throats. Intermittent cavitation noise levels varied between water and sodium, but the rates of change with σ were similar for equivalent geometries. Values of σ_i for the onset of throat cavitation were similar for water and sodium.

c. The intermittent region was absent for wire meshes and σ_i was similar for water and sodium for general cavitation.

d. For a sealing plug with a narrow annular gap the intermittent region was absent and σ_i was sensitive to small geometric imperfections or channel obstructions, making comparison between water and sodium tests difficult.

e. The acoustic technique used was very satisfactory for the determination of incipient cavitation.

8. REFERENCES

1. DELVES P H and SEED G
'Operating Experiences with the Prototype 0.45m^3/sec Sodium Pump'
Institution of Mechanical Engineers Convention of Pumps for Nuclear Power Plants, University of Bath, 1974, paper C104.

2. KOBAYASHI R
'Effect of Cavitation on the Discharge Coefficient of Standard Flow Nozzles'
ASME Journal of Basic Engineering, September 1967, pp 677-685

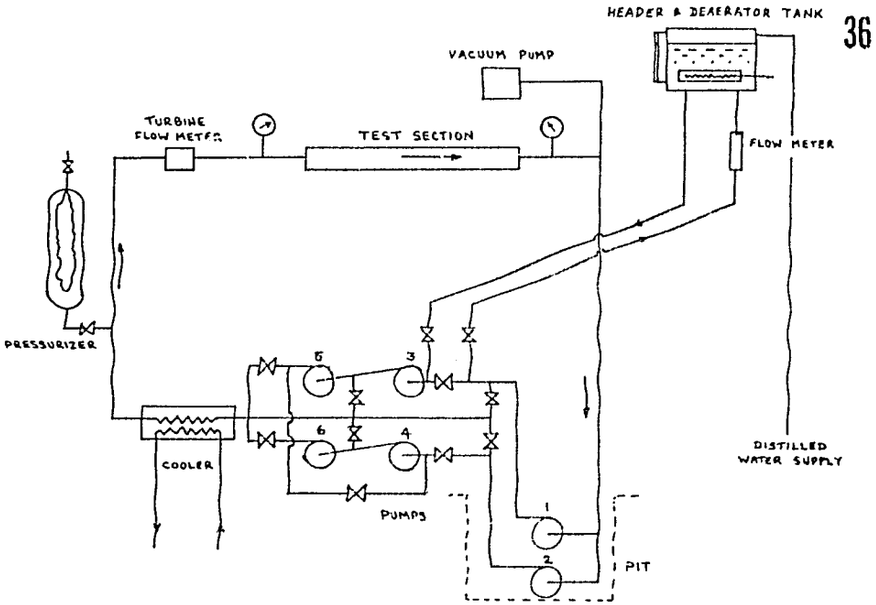

FIG 1 FLOW DIAGRAM OF CAVITATION LOOP (WATER)

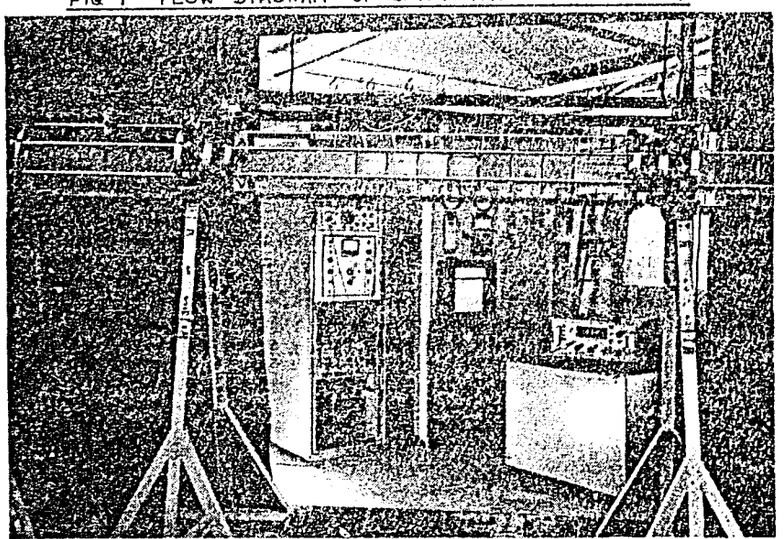

FIG 2 TEST-SECTION : WATER CAVITATION LOOP

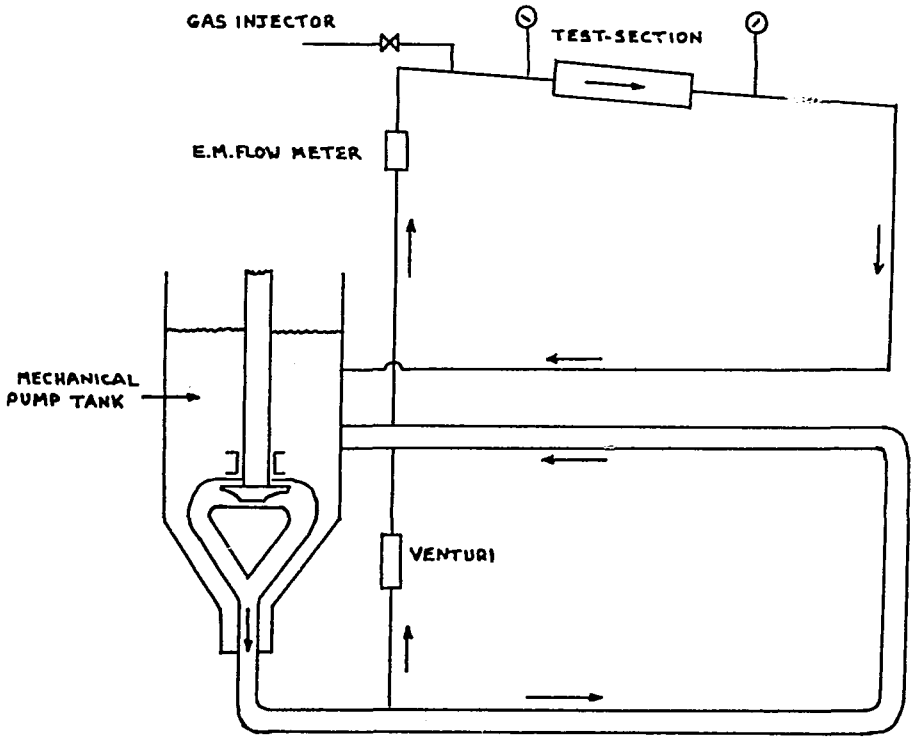

FIG 3 SODIUM CAVITATION LOOP

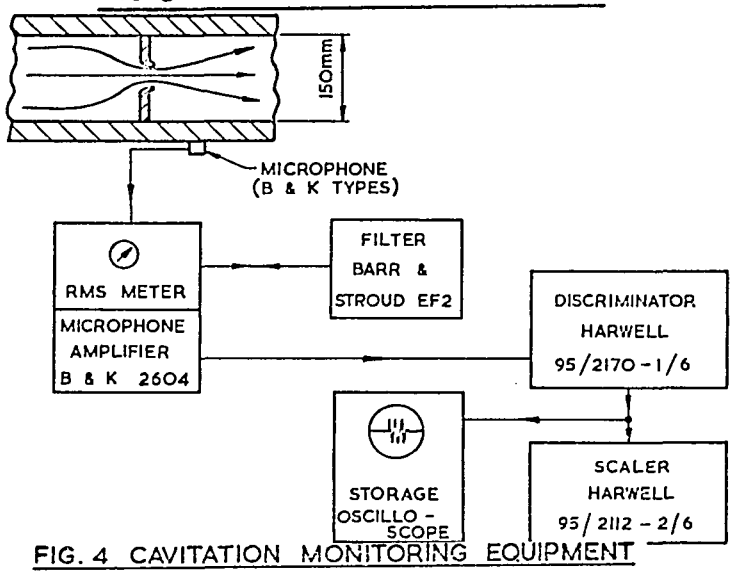

FIG. 4 CAVITATION MONITORING EQUIPMENT

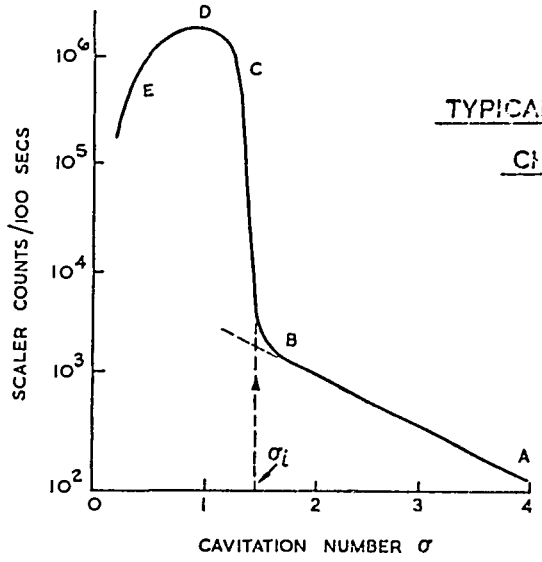

FIG. 5

TYPICAL CAVITATION CHARACTERISTIC

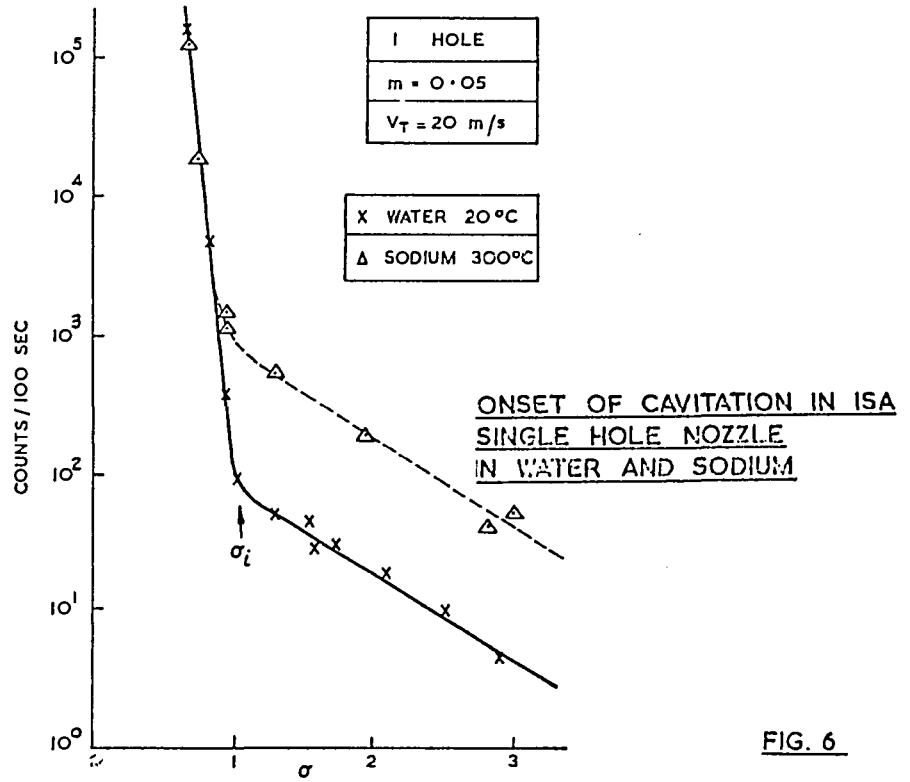

ONSET OF CAVITATION IN ISA SINGLE HOLE NOZZLE IN WATER AND SODIUM

FIG. 6

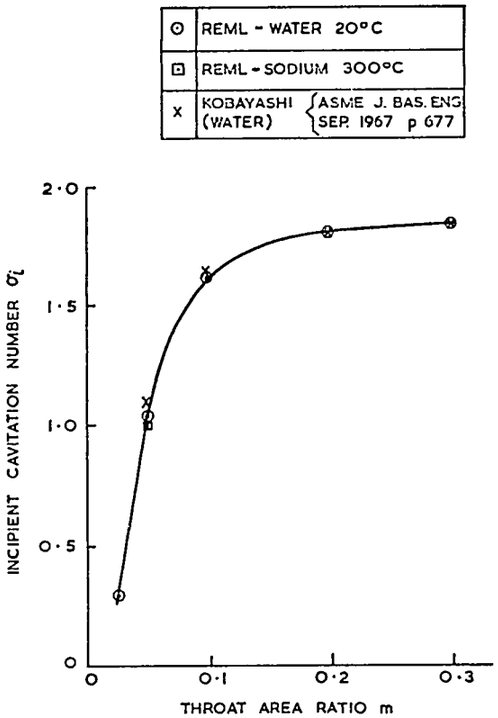

FIG. 7 VARIATION OF INCIPIENT CAVITATION NUMBER WITH THROAT AREA RATIO m FOR SINGLE HOLE NOZZLE

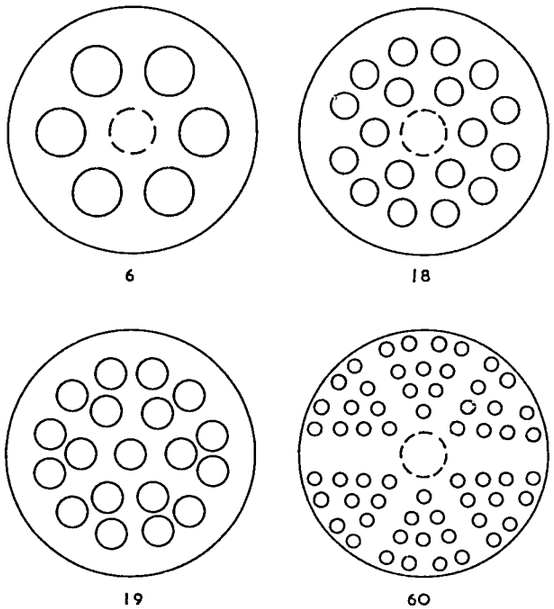

FIG. 8 MULTI-HOLE NOZZLE PLATES

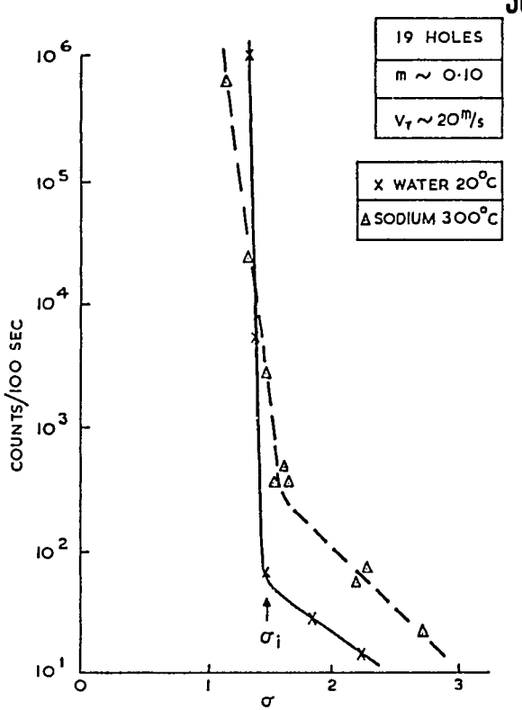

FIG. 9 CAVITATION NOISE FOR 19 HOLE NOZZLE PLATE IN SODIUM AND WATER

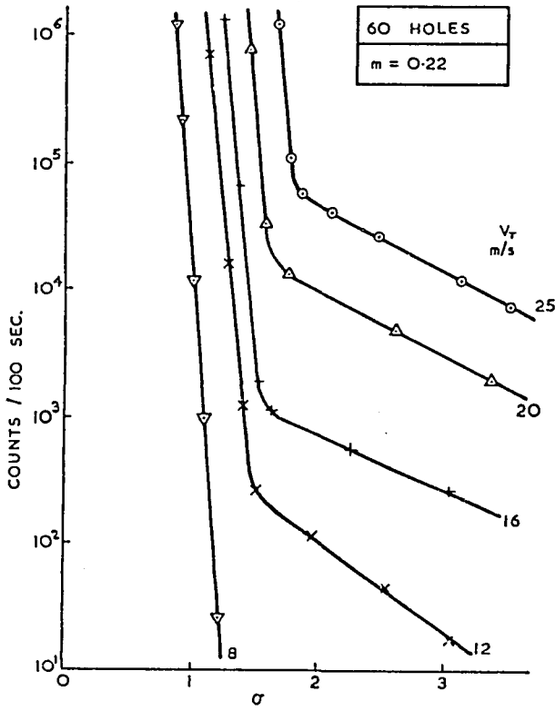

FIG.10 CAVITATION NOISE IN 60 HOLE NOZZLE PLATE FOR VARIOUS WATER VELOCITIES

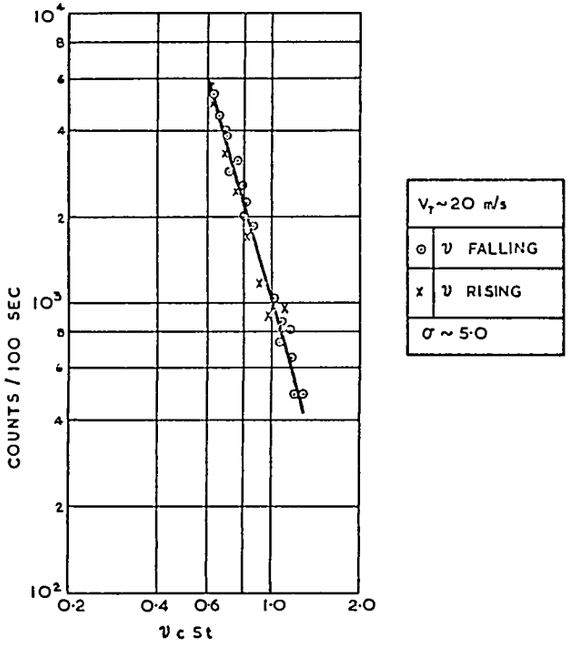

FIG. 11 VARIATION OF COUNT RATE WITH VISCOSITY FOR 60 HOLE PLATE

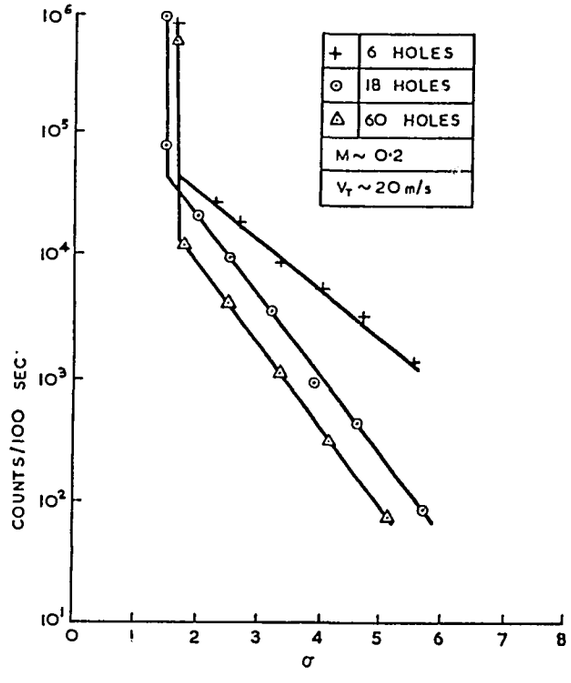

FIG. 12 COMPARISON OF CAVITATION ONSET FOR NOZZLE PLATES WITH 6,18 & 60 HOLES (WATER)

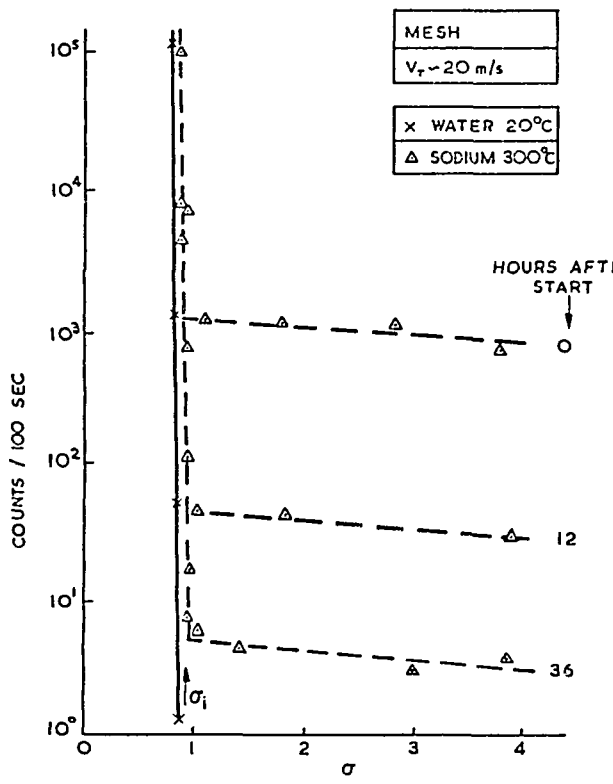

FIG. 13 CAVITATION INCEPTION FOR WIRE MESH IN WATER AND SODIUM

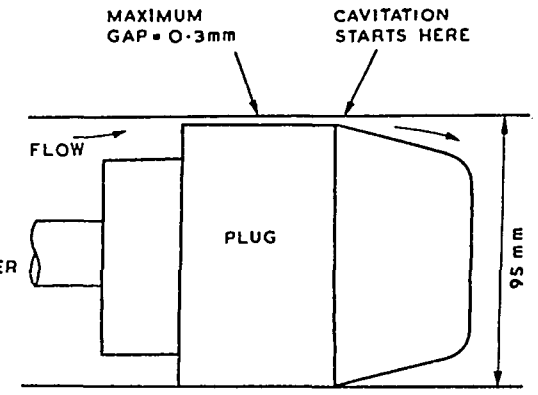

FIG. 14 ANNULAR GEOMETRY OF PLUG IN A TUBE

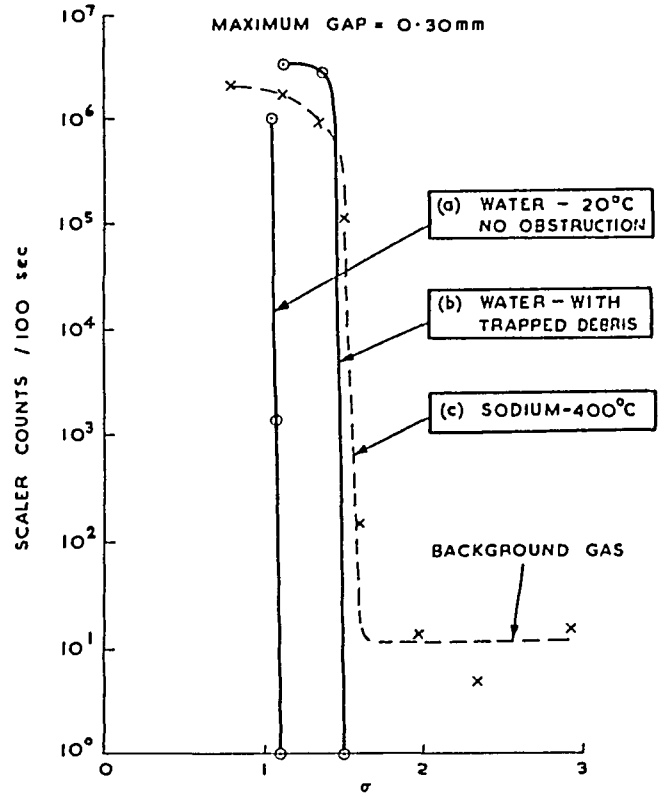

FIG. 15 CAVITATION PERFORMANCE OF PLUG-IN CYLINDER – WATER AND SODIUM

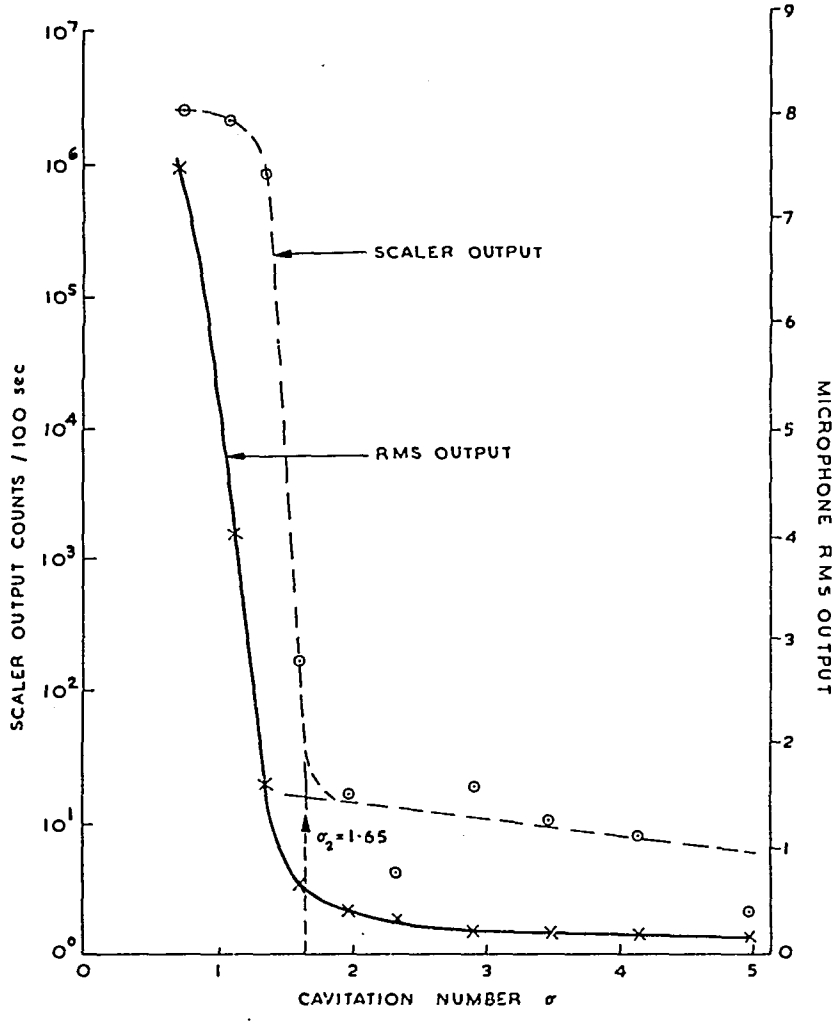

FIG. 16 SODIUM CAVITATION IN 0·3mm ANNULAR GAP
COMPARISON OF MICROPHONE RMS OUTPUT
AND SCALER OUTPUT

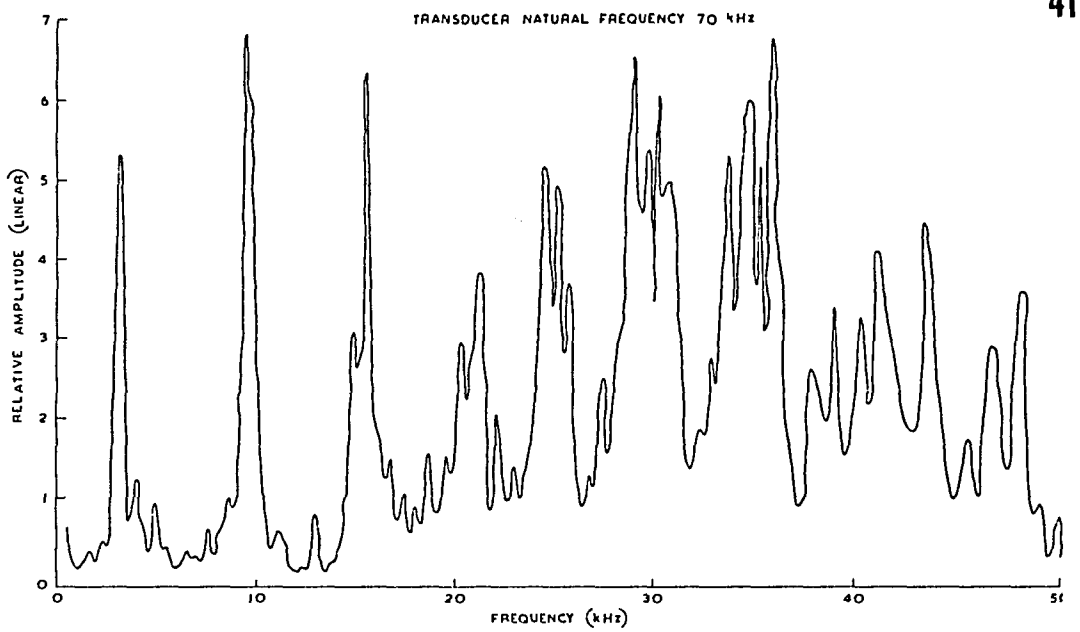

FIG. 17 MICROPHONE FREQUENCY SPECTRUM — ANNULAR GAP
IN SODIUM AT 400°C

4 " Flowrate Regulation Device in PEC Reactor Fuel Element", D. TIRELLI, CNEN, Italy.

Abstract

A calculation method which optimizes a series of sharp-edged constrictions has been defined, to design the PEC reactor fuel element foot and can device. Total pressure drop is divided in each gag to obtain equal cavitation numbers in vena contracta planes.
Water and sodium experimental tests have been carried out for most critical configurations; pressure drop results agree the prediction, while cavitation results are a little spread; some instrumental and modelling improvement activities are now being developed to reduce this uncertainty, to physical-chemical sodium condition variables, in the reactor.